Experimental and finite element modelling of thin sheet hydroforming processes

A. Cherouat[1], M. Ayadi[2], N. Mezghani[2] & F. Slimani[2]

[1] *UTT- GAMMA INRIA, 12 rue Marie Curie, 10010 Troyes, FRANCE*
URL: www.utt.fr *e-mail: abel.cherouat@utt.fr*

[2]*LMSSDT-ESSTT, 5 Av Taha Hussein, Montfleury 1008 Tunis TUNISIA*
URL: www.esstt.rnu.tn *e-mail: mahfoudh.ayadi@esstt.rnu.tn; najehmezghani@yahoo.fr*

ABSTRACT: This paper presents a numerical methodology which aims to improve 3D thin sheet hydroforming processes. This methodology is based on elastoplastic constitutive equations accounting for non-linear anisotropic hardening. The experimental study is dedicated to the identification of material parameters from the global measure of sheet displacement, thickness evolution and internal pressure expansion. Applications are made to study the effect of die shape, anisotropic flow and hardening law on the hydro-formability of sheets.

Key words: Thin sheet, hydroforming, hardening, Anisotropy, Experimental tests.

1 INTRODUCTION

Numerical simulation of metal forming processes is increasingly used by companies as an efficient tool in order to optimize metal forming processes plan before their real fabrication. Nowadays, using the finite element analysis, many numerical models are available to simulate, as accurately as possible, the related phenomena as: material elastoplastic flow, initial anisotropy, contact-friction, thermal effects including the heat exchange sheet-tools, spring-back and residual stresses.

In recent years, sheet hydroforming process is being increasingly used in automotive applications. The advantages of this process compared with traditional manufacturing are considerable and include cost and material savings, weight reduction, quality improvement and better accuracy [1,2].

In free-bulging forming operation, the sheet bulges freely in the die cavity until it contacts the die surface and ensures uniform deformation in the sheet, which improves the dent resistance of the hydroformed part compared with conventional stamped parts. However, micro-defects (damage) can appear inside the formed part due to the large inelastic deformations experienced by the material, die shape, contact-friction and load path conditions. Extensive efforts have been made to understand the yield and flow behavior of cold rolled anisotropic materials experimentally as well as theoretically during hydroforming processes. Many studies have been devoted to the mechanical and numerical modelling of the hydroforming processes using the finite element analysis [3,5], allowing the prediction of the material flow and the contact boundary evolution during the process. However, the main difficulty in many hydroforming processes is to find the convenient control of the evolution of the applied internal pressure and axial forces paths []. This avoids the plastic flow localisation leading to buckling or fracture of the tube during the process.

In this research, the influence of the initial rolling direction deviation of the sheet on the deformation behavior during hydroforming was studied. The elastoplastic constitutive model SWIFFT coupled with Hill's criterion was used to account for isotropic hardening the sheet steel subjected to hydroforming process is analyzed. Numerical simulation was carried out using the explicit finite element code ABAQUS [4]. Predicted displacements versus pressure response were compared to experimental results.

2 THEORETICAL AND EXPERIMENTAL STUDY

Eq. (1) defines the Hill (1948) yield criterion in plane stress state with the material parameters H, G, F, N and the initial yield stress flow σ_y:

$$f = \frac{1}{2}\left[(H+G)\sigma_{11}^2 + (H+F)\sigma_{22}^2 - 2H\sigma_{11}\sigma_{22} + 2N\sigma_{12}^2\right] - \sigma_y^2 = 0 \quad (1)$$

The first identification method only uses the Lankford coefficients $r_{0°}$, $r_{45°}$, $r_{90°}$ (i.e. the ratio between the transversal plastic strain rate and the thickness plastic strain rate) measured during tensile tests at 0°, 45° and 90° from the RD. Eq. 2 is used to identify the Hill material parameters :

$$r_{0°} = \frac{\varepsilon_{22}^p}{\varepsilon_{33}^p} = \frac{H}{G} \quad r_{90°} = \frac{\varepsilon_{11}^p}{\varepsilon_{33}^p} = \frac{H}{F} \quad r_{45°} = \frac{\varepsilon_{22(\alpha=45°)}^p}{\varepsilon_{33}^p} = \frac{2N-F-G}{2(F+G)} \quad (2)$$

Assuming an associated flow rule and denoting the plastic multiplier by λ, the strain tensor and the equivalent plastic strain are given by:

$$\bar{\varepsilon}^p = \sqrt{\frac{4}{3}\varepsilon^p : \varepsilon^p} \qquad \varepsilon^p = \lambda \frac{\partial f}{\partial \sigma}$$

The evolution of the yield surface has been taken into account by means of a Swift hardening law:

$$\sigma_y = K(\varepsilon_0 + \bar{\varepsilon}^p)^n \quad (10)$$

K, n, ε_0, F,G, H and N are the material parameters to be identified numerically using optimisation algorithm. In this formulation, σ_y is chosen to be the uniaxial yield stress associated to the rolling direction. The experimental results of tensile test for different initial rolling directions are presented in Figure 1.

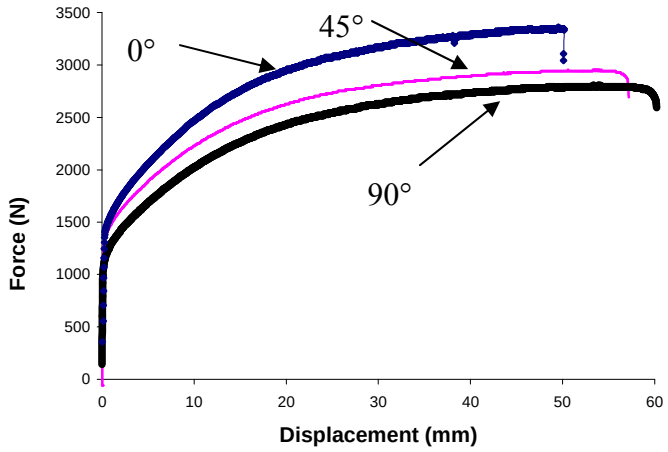

Fig. 1. Global response force versus displacement

Properties of the used material (stainless steel), obtained from the tensile tests, are given in Table 1. Within these coefficients the response (stress versus plastic strain) presents a non linear isotropic hardening with a maximum stress reached $\sigma_{max} = 1110$ MPa for RD=0° case when the hardening is saturated for $\bar{\varepsilon}^p = 0.5$ (see Fig. 2). For RD=45° case the maximum stress reached $\sigma_{max} = 900$ MPa and the hardening is saturated for $\bar{\varepsilon}^p = 0.55$. For RD = 90° the maximum stress is about 890 MPa and the plastic strain at rupture is $\bar{\varepsilon}^p = 0.6$.

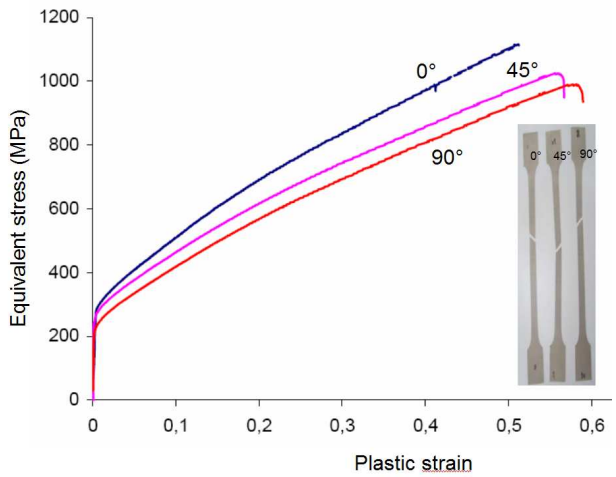

Fig. 2. Local response : stress versus plastic strain (10)

Anisotropic parameters	$r_{0°}$	0.82
	$r_{45°}$	0.92
	$r_{90°}$	0.86

HILL 48 parameters	F	1.52
	G	1.09
	H	0.91
	N	3.245
Flow Stress(MPa)	K (MPa)	1506
	ε_0	0.049
	n	0.5842

Table 1. Mechanical properties of the used material

Figure 3 shows the contours of these anisotropic-hardening yield surfaces under the plane stress state with the principal axes in the rolling 0° and transverse directions 90°. We can nothing that the

convexity of Hill's quadratic yield model for the both initial RD = 0° and 90°.

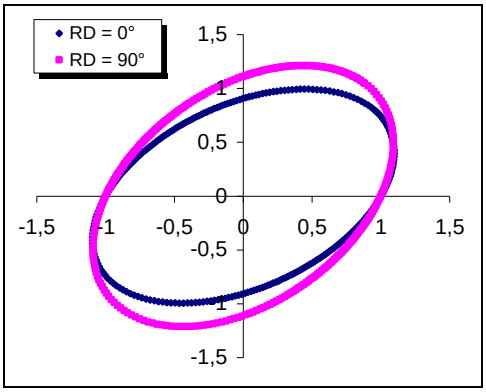

Fig. 3. Yield surfaces with anisotropic hardening.

The square sheet metal subjected to hydroforming is the stainless steel already used in the numerical test. The thickness of the specimen is 0.4 mm, and the clamping length is 50 mm. The boundary coincident with the clamping contour has been fully restrained. The increase of the liquid pressure has been limited to 4.5MPa. The used apparatus is presented in Figure 4. The controlled process parameter is the internal fluid pressure is applied as a uniformly distributed load to the sheet inner surface and is introduced as a linearly increasing function of time (Figure 5). The obtained sheet before and after forming process is presented in Figure 6.

Fig. 4. Experimental apparatus

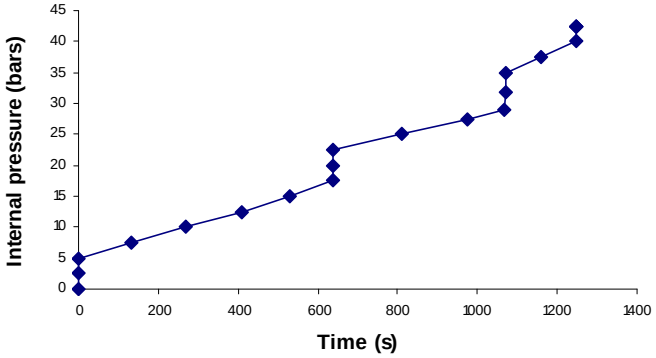

Fig. 5. Imposed loading control

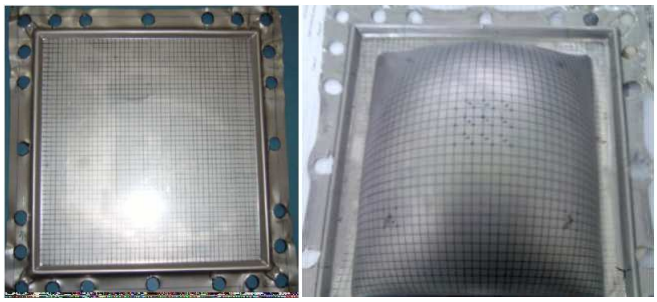

Fig. 6. Sheet before and after hydroforming

3 NUMERICAL RESULTS AND DISCUSIONS

The metal plasticity models in ABAQUS/IMPLCIT use the Hill stress potential for anisotropic behavior. This potential depends only on the deviatoric stress, so the plastic part of the response is incompressible. This means that, in cases where the plastic flow dominates the response (such as limit load calculations or metal forming problems), except for plane stress problems, the finite elements should be chosen so that they can accommodate the incompressible flow. Some examples will be presented in order to test the capability of the elastoplastic model to predict the sheet hydroforming process as well as its ability to study the influence of the anisotropic material. Linear hexahedral finite elements (C3D8R of ABAQUS library) will be used for 3D calculations. Tools (die and blank-holder) are modeled as rigid bodies with their geometry described discretely (R3D4 and R3D3 of ABAQUS library). Figure 7 shows the equivalent stress map and the corresponding deformed mesh after hydroforming.

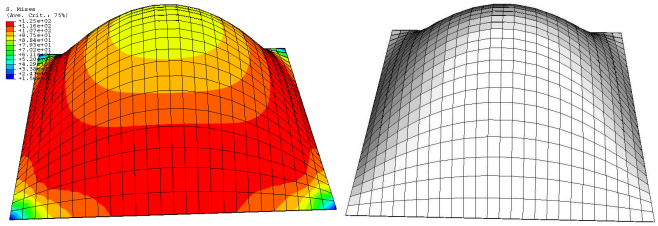

Fig. 7. Stress map and deformed mesh

Figure 8 shows prediction of the displacement at the axial center of sheet versus internal pressure for RD = 0° and RD=45°. The effect of the initial rolling direction is clearly appeared. When *RD*-value is small, the increase in displacement is large (see Figure9).

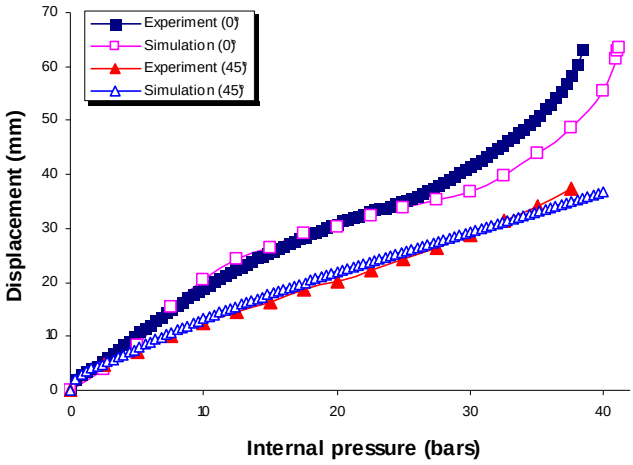

Fig. 8. Displacement versus internal pressure

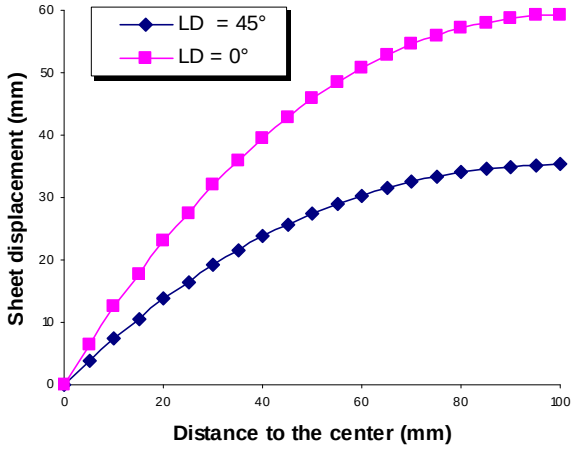

Fig. 9. Sheet profile for RD=0° and RD=45°

The thinning evolution of the deformed sheet is study using non-destructive technique. This technique uses an ultrasonic source to measure the tube thickness variation. It based on the transmission of wave mechanics in the material through a piezoelectric transducer. The transducer is placed on each point of the sheet grid and the values are directly displayed on the screen of the device and stored with an accuracy of a thousandth (0.001mm). The measurements obtained to estimate the sheet thinning along the diagonal and the symmetrical line are compared with numerical values in Figure 10. Good agreement between the experimental values and the predicted results.

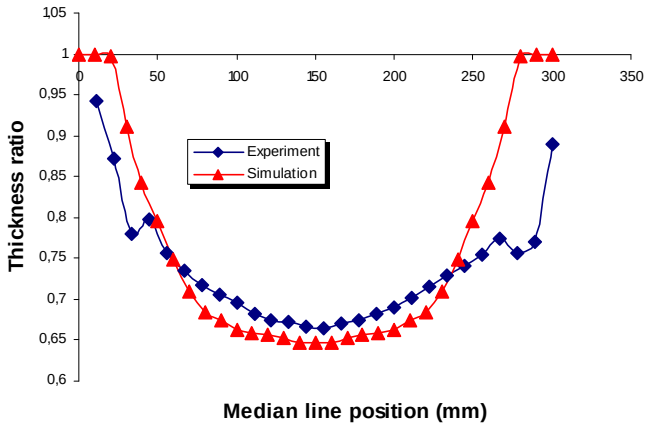

Fig. 10. Thinning of the sheet along the axial line

4 CONCLUSIONS

A constitutive equation accounting for the anisotropic elastoplasticity and hardening has been used to improve numerically a hydroforming of thin sheet. This improvement aims to avoid the initial anisotropy effect on the sheet formability. A work is now in progress which, aims to exploit advanced model to take into account the material degradation during forming process (damage effect).

REFERENCES

1. Asnafi A., Skogsgärdh A., Theoretical and experimental analysis of stroke-controlled tube hydroforming, Materials Science & Engineering 2000; vol. 279 : 95-110

2. Nakamura S., Sigiura H., Onoe H., Ikemoto K., hydromechanical drawing of automotive parts, Journal of Materials Processing Technology 1994; vol. 46 : 491-503

3. Zhang S.H., Danckert J., Development of hydromechanical deep drawing, Journal of Materials Processing Technology 1998; vol. 83 : 14-25

4. ABAQUS, Theory Manual, Version 6.5, Hibbit, Karson & Sorensen, Inc., 2005.

5. Comsa, G. Cosovici, P. Jurco, L. Paraianu and D. Banabic Simulation of the hydroforming process using a new orthotropic yield criterion, Journal of Materials Processing Technology, 2004, vol. 157-158 : 67-74

6. A. Cherouat, K. Saanouni and Y. Hammi Numerical improvement of thin tubes hydroforming with respect to ductile damage, I. J. of Mechanical Sciences, 2002, vol. 44: 2427-2446